Received September 17, 2019, accepted October 7, 2019, date of publication October 21, 2019, date of current version October 31, 2019.

Digital Object Identifier 10.1109/ACCESS.2019.2948656

Modeling and Analysis of Two-Way Relay Networks: A Joint Mechanism Using NOMA and Network Coding

FANBO WEI[1,2], TING ZHOU[1], (Member, IEEE), TIANHENG XU[1], (Member, IEEE), AND HONGLIN HU[1], (Senior Member, IEEE)

[1]Shanghai Advanced Research Institute, Chinese Academy of Sciences, Shanghai 201210, China
[2]School of Electronic, Electrical and Communication Engineering, University of Chinese Academy of Sciences, Beijing 100049, China

Corresponding author: Honglin Hu (hlhu@ieee.org)

This work was supported in part by the National Natural Science Foundation of China under Grant 61801461 and Grant 61801460, in part by the Strategical Leadership Project of Chinese Academy of Sciences under Grant XDC02070800, and in part by the Shanghai Municipality of Science and Technology Commission Project under Grant 18XD1404100 and Grant 17QA1403800.

ABSTRACT As a promising technology, non-orthogonal multiple access (NOMA) enhances spectral efficiency and system capacity by allocating the same resource to multiple users. Network coding (NC) has the advantages of compressing data and high spectral efficiency, and it plays a crucial role in two-way relay networks. However, conventional two-way relay networks suffer from throughput limitations due to the use of OMA scheme. In this paper, we utilize a hybrid concept to design a two-way relaying system (namely Hybrid-TWRS) which combines NOMA and NC. Furthermore, we investigate the size-mismatch problem caused by asymmetric channel in the NOMA scheme and propose a bit-match scheme and a symbol-match scheme based on the Hybrid-TWRS. Theoretical derivation and numerical results demonstrate that the proposed method distinctly outperforms both (i) traditional two-way relaying system with OMA in the uplink and NC in the downlink (namely NC-TWRS); and (ii) NOMA-based two-way relaying system (namely NOMA-TWRS).

INDEX TERMS Two-way relay network, non-orthogonal multiple access (NOMA), network coding, size-mismatch problem, throughput performance.

I. INTRODUCTION

IN recent years, non-orthogonal multiple access (NOMA) has attracted extensive academic interest due to its massive connectivity and low signaling cost. These features are also the main advantages of NOMA compared with orthogonal multiple access (OMA) [1]–[3]. In conventional mobile communication systems, radio resources are always orthogonal in time-, frequency-, code-, or spatial domain. By contrast, in the NOMA scheme, multiple users can share the same resource. Therefore, significant enhancements of spectral efficiency and system capacity can be achieved by NOMA compared with OMA techniques [4], [5].

NOMA is suitable for serving users of different channel conditions in the same resource [6], [7]. It is also widely recognized that the maximum attainable system capacity can be achieved in downlink channels of NOMA [19]. Although recent research has demonstrated that NOMA has vast potentials, few studies have taken round trip transmission into consideration to evaluate the entire system performance. Specifically, most existing research models are one-way, i.e., either uplink or downlink [8], [9].

Wireless two-way relay network is a basic network framework in communication systems [10], [11]. It consists of one relay node and two terminal nodes. When the channel condition between the two terminal nodes is poor, the relay node helps them to complete a better transmission. By combining the two technologies of coding and routing, network coding (NC), proposed by Ahlswede and other scholars in 2000 [12], has been applied to two-way relay network. Instead of adopting simple amplification or forwarding, the relay node encodes the information to be transmitted by using NC. Hence, the NC scheme brings performance gain in downlink two-way relaying system. However, conventional two-way

The associate editor coordinating the review of this manuscript and approving it for publication was Mojtaba Vaezi.

This work is licensed under a Creative Commons Attribution 4.0 License. For more information, see http://creativecommons.org/licenses/by/4.0/

relaying do not apply the NOMA scheme to the uplink [13], [14], which did not reach their full potential in improving system capacity.

Previous studies have applied NOMA to two-way relay networks. More precisely, the upper bound of capacity for multi-user MIMO (MU-MIMO) NOMA in the two-way relaying system is analyzed in [15]. Zheng *et al.* [16] have investigated the secure NOMA-based two-way relay network with the full-duplex relay. In addition, Yue *et al.* [17] proposed the closed-form expression of outage probability for NOMA-based two-way relaying (TWR-NOMA) with imperfect SIC and perfect SIC. Besides, they show that the outage performance of TWR-NOMA is superior to TWR-OMA in the low signal-to-noise ratio (SNR) regime. All the above references study the application of NOMA in both the uplink and the downlink. However, the high complexity of system-level signal detection in NOMA-based two-way relaying needs to be considered. Besides, the error propagation caused by successive interference cancellation (SIC) technique on both the relay node and the terminal node cannot be ignored either.

Inspired by the benefits of NOMA and NC, we aim to further improve system capacity by investigating a hybrid concept that combines those two technologies in a round trip transmission. However, due to the asymmetric channel in NOMA scheme, a mismatch problem exists between the size of two users' symbol sequences or between the size of two users' bit sequences when applying adaptive modulation and coding (AMC). The above discussions motivate us to design a hybrid two-way relaying method and propose solutions to solve the size-mismatch problem of the method. The main contributions of our work can be summarized as follows.

- We utilize a hybrid two-way relaying system (namely Hybrid-TWRS), which applies the NOMA scheme in the uplink and multicasts the messages in the form of network coding in the downlink. By investigating both the multiplexing gain of NOMA and the compressing gain of network coding, Hybrid-TWRS can achieve higher system capacity compared to the conventional two-way relaying system (namely NC-TWRS). To demonstrate the joint gain of NOMA and NC, we take the only-NOMA-based two-way relaying system (namely NOMA- TWRS) as a comparison.
- For both the uplink and the downlink in two-way relaying, we model the three methods and derive their throughput expressions. Moreover, the theoretical throughput and detection complexity of the three methods are compared. The results show that the proposed method Hybrid-TWRS achieves lower detection complexity than that of NOMA- TWRS method. More precisely, 25% complexity can be reduced.
- For the size-mismatch problem, two different matching schemes for information sequences are elaborated: (i) bit-match scheme; and (ii) symbol-match scheme. Furthermore, we compare the performance of the two schemes and give the recommended scheme for Hybrid-TWRS, i.e., a more suitable scheme is selected and utilized in the final simulation.
- We analyze the performance of the proposed method by simulations. Also, the superiorities of Hybrid-TWRS in bit-error-rate (BER)/block-error-rate (BLER) and throughput performance are confirmed.

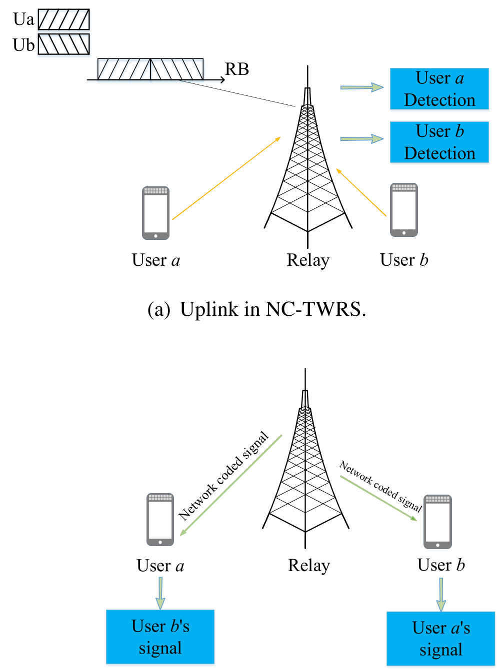

(a) Uplink in NC-TWRS.

(b) Downlink in NC-TWRS.

FIGURE 1. Conventional two-way relaying system (NC-TWRS).

The rest of this paper is organized as follows. In Section II, the system model of the conventional two-way relaying method NC-TWRS is first introduced, then the NOMA-based two-way relaying NOMA-TWRS is described mathematically. After that, in Section III, we first demonstrate the proposed model Hybrid-TWRS, then we derive and compare the theoretical system performance of the three techniques. In Section IV, we investigate the two different size-match transmission schemes in the asymmetric channel. Then simulation results and the corresponding performance analysis are exhibited in Section V, followed by the conclusions and the future directions of this work drawn in Section VI.

II. SYSTEM MODEL AND PROBLEM FORMULATION

In this section, the conventional two-way relaying and the NOMA-based two-way relaying are depicted in Fig. 1 and Fig. 2, respectively. The single relay node R, regarded as a base station (BS) in this paper, is located in the center of the cell network. Notations h_a and h_b are denoted as the channel coefficients of terminal nodes UE_a and UE_b, respectively. We consider that UE_b is closer to the relay node than UE_a, and the channel condition of UE_b is better than that of UE_a, i.e., $|h_b|^2 > |h_a|^2$.

For clear description, we denote that x_i is the data bit sequence, while c_i and c_i' are the channel coded bit sequences of UE_i in the uplink and the downlink respectively. Notations P_i and P' stand for the transmission power of UE_i and the relay respectively. Notations S_i and S' mean the transmitted symbols in the uplink and the downlink, $i \in \{a, b\}$. In addition, G_i denotes the MMSE (Minimum Mean Square Error) equalization coefficient of UE_i. X denotes the network coded bit sequence by XOR operation.

A. CONVENTIONAL TWO-WAY RELAYING (NC-TWRS)

Fig. 1 illustrates the transmission of NC-TWRS. The system model of NC-TWRS can be shown mathematically as follows.

1) In the uplink, users have their own individual resource blocks (RBs). The received signals at the base station are represented by

$$y_a = h_a\sqrt{P_a}S_a + w_a, \tag{1}$$

and

$$y_b = h_b\sqrt{P_b}S_b + w_b. \tag{2}$$

Here, user UE_i transmits the signal S_i, w is the additive white Gaussian noise (AWGN) with zero mean and variance σ_w^2.

2) The detected symbol at the BS can be formulated as

$$\hat{S}_i = G_i(h_i\sqrt{P_i}S_i + w_i). \tag{3}$$

Afterwards, the signal of UE_i is decoded by demodulation and channel decoding: $\hat{S}_i \to \hat{c}_i \to \hat{x}_i$. $\hat{c}_i$ and $\hat{x}_i$ represent the detected channel decoded bit sequence and the detected bit sequence of UE_i, respectively.

3) The BS then encodes the decoded bit sequences of two users by using XOR operation as follows.

$$X = \hat{x}_a \oplus \hat{x}_b. \tag{4}$$

The network coded bit sequence X is then mapped to the transmitted symbols for two users through channel coding and modulation: $X \to c' \to S'$.

4) In the downlink, the BS broadcasts the network coded symbol S' to the users. At the terminal node, the received signal of UE_i is represented by

$$y_i = h_i\sqrt{P'}S' + w_i. \tag{5}$$

B. NOMA-BASED TWO-WAY RELAYING (NOMA-TWRS)

We consider an only-NOMA based two-way relaying (NOMA-TWRS). This method achieves resource sharing of two terminal users on the same RB by applying NOMA scheme on both the uplink and the downlink.

1) In the uplink scenario as Fig. 2(a) illustrates, the signals of two nodes are directly superimposed. For simplicity of the system model, we assume that the channel conditions of users are significantly different. Hence the transmit power of the users in the uplink dose not have to be different in this paper,

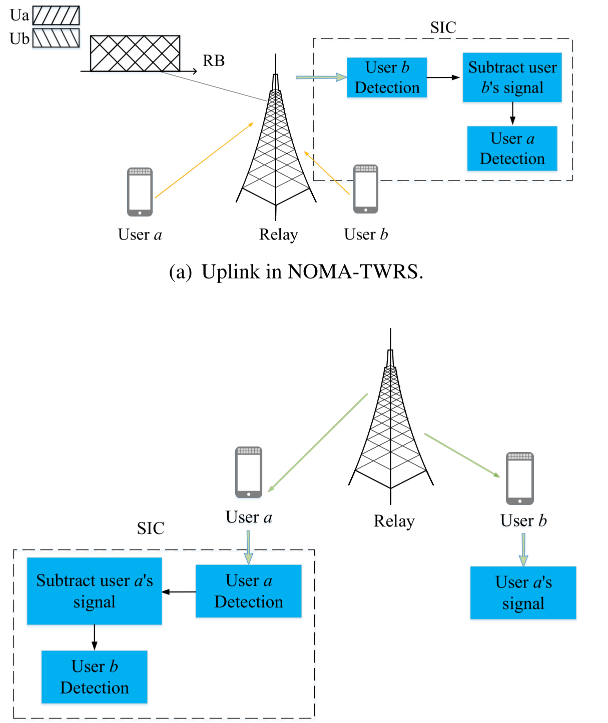

(a) Uplink in NOMA-TWRS.

(b) Downlink in NOMA-TWRS.

FIGURE 2. **NOMA-based two-way relaying system (NOMA-TWRS).**

i.e., $P_a = P_b = 1$ [20]. The received signal at the BS can be given by

$$y = h_aS_a + h_bS_b + w. \tag{6}$$

2) Then, SIC technique is applied to the base station. The BS decodes signals of UE_a and UE_b in two stages. Particularly, in the first stage, the signal of UE_b (i.e., the near user) is detected, treating the signal of UE_a as noise. The detected symbol of UE_b is represented as

$$\hat{S}_b = G_b(h_aS_a + h_bS_b + w). \tag{7}$$

The data bit sequence of UE_b can also be decoded by demodulation and channel decoding: $\hat{S}_b \to \hat{c}_b \to \hat{x}_b$.

In the next stage, the BS subtracts the detected signal S_b from the received signal, then the detected symbol S_a is obtained by

$$\hat{S}_a = G_a(y - h_b\hat{S}_b). \tag{8}$$

Furthermore, the BS decodes the signal of UE_a: $\hat{S}_a \to \hat{c}_a \to \hat{x}_a$.

3) Fig. 2(b) demonstrates the downlink scenario. After $\hat{x}_i$ is remapped to the symbol S_i', with the help of superposition coding and power allocation at the BS, the received signal can be written as

$$y_i = h_iS' + w_i. \tag{9}$$

Here S' is the superposed signal at the BS, which satisfies $S' = \sqrt{P'\beta_a}S_a' + \sqrt{P'\beta_b}S_b'$. Note that β_i denotes the fraction of the power P' assigned to the user UE_i, subject to the constraints on $\beta_a + \beta_b = 1$ and $\beta_a > \beta_b$.

4) In the downlink, the order of decoding is reversed compared to the uplink. The optimal order for decoding in the downlink is in the order of the increasing channel gain. This is because the throughput of the near user UE_b is bandwidth-limited rather than power-limited. Besides, superposition coding with the far user UE_a allows UE_b to use the full bandwidth while being allocated only a small amount of transmission power because of power sharing with UE_a [18]. At the terminal node UE_a, the detected signal can be given by

$$\hat{S_a'} = G_a(h_a S' + w_a). \tag{10}$$

Then UE_a subtracts the signal $\hat{S_a'}$ from the received signal y_i. After that, the detected signal of UE_b at the node UE_a is written as

$$\hat{S_b'} = G_a(y_a - h_a \hat{S_a'}). \tag{11}$$

Similarly, by utilizing the SIC technique, the signal of UE_a can also be decoded at node UE_b. According to the above process, the exchange of information is achieved between UE_a and UE_b.

From these two methods, it can be observed that the superiority of the NOMA scheme has the opportunity to be applied to two-way relaying. Additionally, different from the above NOMA-TWRS system, we utilize a hybrid concept to combine NOMA and network coding to improve detection complexity and minimize the impact of error propagation. The proposed model and theoretical derivation are given in the following section.

III. PROPOSED METHOD AND SYSTEM PERFORMANCE ANALYSIS

In this section, the system formulations of our proposed two-way relaying method Hybrid-TWRS are first given. Then we derive the achievable rates for the proposed method and two other counterparts NC-TWRS and NOMA-TWRS. Finally, we compare the detection complexity of the three systems.

A. PROPOSED TWO-WAY RELAYING (HYBRID-TWRS)

The particular process of our proposed method Hybrid-TWRS can be shown mathematically as follows.

1) The uplink scenario in Hybrid-TWRS is shown in Fig. 3(a). With the assumption that $P_a = P_b = 1$, the BS receives the signal from the paired users UE_a and UE_b:

$$y = h_a S_a + h_b S_b + w. \tag{12}$$

2) Then the BS decodes the signals of UE_b and UE_a by using SIC technique:

$$\hat{S_b} = G_b(h_a S_a + h_b S_b + w), \tag{13}$$

and

$$\hat{S_a} = G_a(y - h_b \hat{S_b}). \tag{14}$$

The bit sequences of UE_b and UE_a can be obtained respectively: $\hat{S_b} \to \hat{c_b} \to \hat{x_b}$; $\hat{S_a} \to \hat{c_a} \to \hat{x_a}$.

3) Fig. 3(b) reveals the downlink scenario of Hybrid-TWRS. The BS encodes the detected bit sequences of two users by XOR operation:

$$X = \hat{x_a} \oplus \hat{x_b}. \tag{15}$$

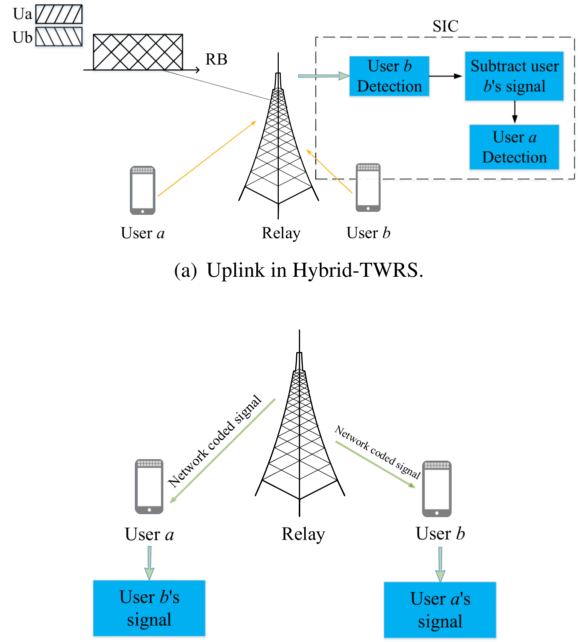

FIGURE 3. Hybrid two-way relaying system (Hybrid-TWRS).

After that, the BS maps the network coded signal to the transmitted symbol ($X \to c' \to S'$) and sends it to users. The received signal of UE_i is given by

$$y_i = h_i \sqrt{P'} S' + w_i. \tag{16}$$

4) The detected symbol at terminal nodes can be obtained as

$$\hat{S_i'} = G_i(h_i \sqrt{P'} S' + w_i). \tag{17}$$

The data bit sequence of UE_i can also be decoded by demodulation and channel decoding: $\hat{S_i'} \to \hat{c_i} \to \hat{X_i}$. We denote that $\hat{c_i}$ and $\hat{X_i}$ are the channel decoded bit sequence and the detected bit sequence of UE_i, respectively.

5) At the terminal nodes, UE_i decodes the detected bit sequence $\hat{X_i}$ by XOR operation and finally receives the messages from another user. At UE_a side and UE_b side, the detected bit sequence can be formulated respectively by

$$\hat{x_b'} = \hat{X_a} \oplus x_a, \tag{18}$$

and

$$\hat{x_a'} = \hat{X_b} \oplus x_b. \tag{19}$$

Based on the above process, messages are exchanged in Hybrid-TWRS.

B. SUM THROUGHPUT ANALYSIS IN UPLINK

The system throughput is the sum of the data rates of all terminals transmitted to the network. For both OMA and NOMA, which is the only difference between NC-TWRS and Hybrid-TWRS, two users are assumed to share the entire 1 Hz BW simultaneously. Note that whether SIC is perfect does not affect the comparison results. Thus, without loss of generality, perfect SIC is used in the derivation of theoretical throughput in this paper. From the definition of throughput and the Shannon equation, the throughput of uplink OMA can be expressed as [19]

$$R_a^{\text{OMA,U}} = \alpha \log_2(1 + \frac{P_a|h_a|^2}{\sigma_n^2}), \tag{20}$$

and

$$R_b^{\text{OMA,U}} = (1-\alpha)\log_2(1 + \frac{P_b|h_b|^2}{\sigma_n^2}), \tag{21}$$

where α denotes the resource allocation coefficient, subject to the constraint on $0 < \alpha < 1$. Also, σ_n^2 represents the AWGN. The power of users satisfies: $P_a = P_b$.

According to the assumption that $|h_b|^2 > |h_a|^2$, the signal of UE_b is first decoded at the BS. The throughput of two users and the sum throughput in uplink NOMA can be formulated as

$$R_a^{\text{NOMA,U}} = \log_2(1 + \frac{P_a|h_a|^2}{\sigma_n^2}), \tag{22}$$

$$R_b^{\text{NOMA,U}} = \log_2(1 + \frac{P_b|h_b|^2}{P_a|h_a|^2 + \sigma_n^2}), \tag{23}$$

$$R_{\text{sum}}^{\text{NOMA,U}} = \log_2(1 + \frac{P_a|h_a|^2 + P_b|h_b|^2}{\sigma_n^2}), \tag{24}$$

respectively. Let us denote the transmit SNR at the BS by ρ and assume that the power of users in uplink NOMA scheme is same as that of OMA users.

Taking the special case to analyze the throughput of NOMA and OMA in the uplink: when SNR is rather high, and the RBs of two users are assumed equally allocated to each other. Then the throughput of OMA and NOMA in uplink can be written as [20]

$$\begin{aligned} R_{\text{sum}}^{\text{OMA,U}} &= \frac{1}{2}\log_2(1 + \frac{P_a|h_a|^2}{\sigma_n^2} + \frac{P_b|h_b|^2}{\sigma_n^2} + \frac{P_a^2|h_a|^2|h_b|^2}{\sigma_n^4}) \\ &= \frac{1}{2}\log_2(\rho^2(\frac{1}{\rho^2} + \frac{|h_a|^2}{\rho} + \frac{|h_b|^2}{\rho} + |h_a|^2|h_b|^2)) \\ &\approx \frac{1}{2}\log_2(\rho^2|h_a|^2|h_b|^2). \end{aligned} \tag{25}$$

and

$$\begin{aligned} R_{\text{sum}}^{\text{NOMA,U}} &= \log_2(\rho(\frac{1}{\rho} + |h_a|^2 + |h_b|^2)) \\ &\approx \log_2(\rho(|h_a|^2 + |h_b|^2)). \end{aligned} \tag{26}$$

Consequently, the throughput gain of NOMA over OMA can be given by

$$R_{\text{sum}}^{\text{Gain,U}} = R_{\text{sum}}^{\text{NOMA,U}} - R_{\text{sum}}^{\text{OMA,U}} = \log_2(\frac{|h_b|}{|h_a|} + \frac{|h_a|}{|h_b|}). \tag{27}$$

Since we have $|h_b| > |h_a| > 0$, the throughput of NOMA is higher than that of OMA in uplink, i.e.,

$$R_{\text{sum}}^{\text{NOMA,U}} > R_{\text{sum}}^{\text{OMA,U}}. \tag{28}$$

C. SUM THROUGHPUT ANALYSIS IN DOWNLINK

In the downlink, which is the only difference between Hybrid-TWRS and NOMA-TWRS. Uplink NOMA and downlink NOMA have two significant differences. In downlink NOMA, SIC technique is adopted to first decode the signal of UE_a with higher transmit power, then the decoded signal of UE_a is subtracted from the received signal, and UE_b with lower transmit power is decoded. With the above analysis, the throughput of two-user downlink NOMA can be written as

$$R_a^{\text{NOMA,D}} = \log_2(1 + \frac{P'_a|h_a|^2}{P'_b|h_a|^2 + \sigma_n^2}), \tag{29}$$

and

$$R_b^{\text{NOMA,D}} = \log_2(1 + \frac{P'_b|h_b|^2}{\sigma_n^2}). \tag{30}$$

Here, the power of users is expressed as: $P'_a = \beta_a P'$ and $P'_b = \beta_b P'$. β_a and β_b denote the power allocation coefficients of UE_a and UE_b, respectively, and they satisfy: $\beta_a + \beta_b = 1$.

Then, the downlink network coding is considered. Since the BS applies the XOR operation to the data of two users, the signals of two users also share the same RB. The throughput of the downlink network coding can be given by

$$R_a^{\text{NC,D}} = \log_2(1 + \frac{P'|h_a|^2}{\sigma_n^2}), \tag{31}$$

and

$$R_b^{\text{NC,D}} = \log_2(1 + \frac{P'|h_b|^2}{\sigma_n^2}). \tag{32}$$

Since $\beta_a = 1 - \beta_b < 1$, and by (29) and (31), we have

$$P'_a|h_a|^2 = \beta_a P'|h_a|^2 < P'|h_a|^2, \tag{33}$$

and

$$P'_b|h_a|^2 + \sigma_n^2 > \sigma_n^2. \tag{34}$$

Thus, we have

$$R_a^{\text{NC,D}} > R_a^{\text{NOMA,D}}. \tag{35}$$

Following the similar operations as the above, it can be observed from (30) and (32) that

$$P'_b|h_b|^2 = \beta_b P'|h_b|^2 < P'|h_b|^2, \tag{36}$$

hence we have

$$R_b^{\text{NC,D}} > R_b^{\text{NOMA,D}}. \tag{37}$$

Using (35) and (37), we can further conclude that

$$R_{\text{sum}}^{\text{NC,D}} > R_{\text{sum}}^{\text{NOMA,D}}. \tag{38}$$

TABLE 1. Detection complexity for uplink and downlink.

Name	real-valued multiplications	real-valued additions
NOMA-TWRS in uplink	$4N^3 + 24N^2$	$4N^3 + 14N^2$
NC-TWRS in uplink	$4N^3 + 24N^2$	$4N^3 + 14N^2$
Hybrid-TWRS in uplink	$4N^3 + 24N^2$	$4N^3 + 14N^2$
NOMA-TWRS in downlink	$4N^3 + 24N^2$	$4N^3 + 14N^2$
NC-TWRS in downlink	$2N^3 + 12N^2$	$2N^3 + 7N^2$
Hybrid-TWRS in downlink	$2N^3 + 12N^2$	$2N^3 + 7N^2$

Besides, the theoretical throughput of Hybrid-TWRS and NC-TWRS can also be compared using (28). Therefore, we believe that the theoretical system throughput of Hybrid-TWRS is higher than that of NC-TWRS. Furthermore, for Hybrid-TWRS and NOMA-TWRS, the conclusion can be obtained by (38): the theoretical achievable rate of Hybrid-TWRS is higher than that of NOMA-TWRS.

Based the above, derivation results demonstrate that uplink NOMA is highly effective in terms of throughput compared with uplink OMA. Besides, downlink network coding utilizes its advantages of compressing data to achieve a better performance than downlink NOMA. Thus, as a promising model, our proposed method Hybrid-TWRS has the maximum theoretical system-level throughput compared with NC-TWRS technique and NOMA-TWRS technique.

D. DETECTION COMPLEXITY ANALYSIS

To verify the practicability of the proposed method, we calculate the detection complexity of the three systems according to the number of times they perform MMSE detection in the uplink and the downlink. For the classical MMSE detection algorithm, by applying the method in [21], its complexity can be given by $2N^3+12N^2$ for multiplications and $2N^3+7N^2$ for additions, respectively. Notation N is the number of detected symbols in a frame. Consequently, the detection complexity of both the uplink and the downlink for the three systems are presented in Table 1.

It can be observed that the detection complexity of uplink NOMA approximates that of OMA. This is because NOMA applies SIC technique at the BS. Specifically, the MMSE detection is performed twice per frame, and each time the receiver decodes the signal of one user only. While for OMA, two users apply the orthogonal resource to transmit their signals. Thus, the BS performs MMSE detection twice too. However, for downlink network coding, since it benefits from XOR operation, the scheme only performs MMSE detection once for one user. Consequently, the detection complexity of downlink NC is lower than that of downlink NOMA which carries out MMSE detection twice at one terminal node.

In summary, the detection complexity of Hybrid-TWRS is reduced by about 25% compared to that of NOMA-TWRS.

IV. BIT-MATCH SCHEME AND SYMBOL-MATCH SCHEME IN HYBRID-TWRS

Recall the application scenario of power-domain NOMA, to minimize inter-user interference (IUI) and thus to maximize system throughput, two users with significant channel

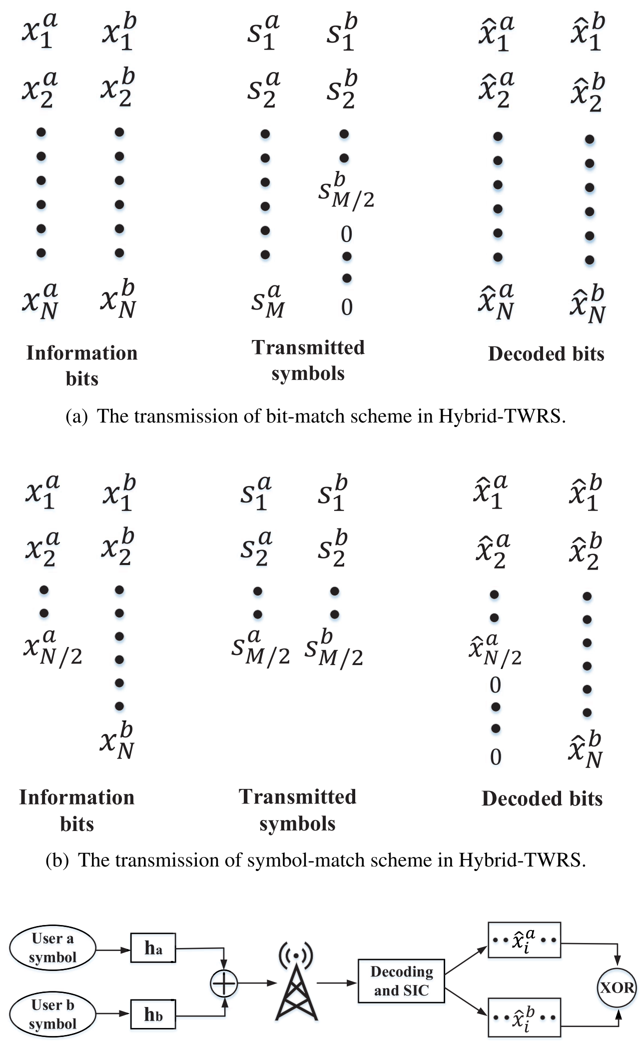

(a) The transmission of bit-match scheme in Hybrid-TWRS.

(b) The transmission of symbol-match scheme in Hybrid-TWRS.

(c) The transmission processing in Hybrid-TWRS.

FIGURE 4. Illustration of the different transmission schemes in Hybrid-TWRS.

differences need to be paired. Nevertheless, the asymmetric channel in uplink NOMA will most likely lead to the difference in modulation and coding schemes (MCS) between the paired users when AMC is applied [22]. Thus, without loss of generality, in this paper we only consider the two NOMA users who have different modulation methods [23].

Since the symbol sequences of the two users are naturally superimposed in the uplink NOMA, they need to be the same size for a completely non-orthogonal transmission. However, in the downlink the relay node XOR the decoded bit sequences of two users, which also requires the original bit sequences of two users to be the same size. Consequently, the different modulation will eventually lead to a mismatch, which between the size of the two users' symbol sequences in the uplink or between the size of the two users' bit sequences in the downlink.

According to the size-mismatch problem in the Hybrid-TWRS, we propose the bit-match scheme, which meets the size requirements of the two users' bit sequences in the downlink. Besides, the symbol-match scheme is investigated to satisfy the size requirements of the two users' symbol sequences in the uplink. The analysis of the two schemes is also given in this section.

A. TRANSMISSION OF BIT-MATCH SCHEME

In this paper, we assume that the modulation order of the two users differs by one (user 1: BPSK, user 2: QPSK). Fig. 4 (a) displays the bit-match scheme for Hybrid-TWRS. In bit-match scheme, since different modulation methods are adopted, two data streams of the same size x_1 and x_2 are mapped to two symbol sequences of different sizes s_1 and s_2 respectively after channel coding. Zero-padding is then applied to the sequence with a smaller number of symbols to achieve the superposition of signals. Given the above operation, OMA and NOMA coexist in the uplink Hybrid-TWRS. Additionally, XOR operation is used at the BS with the two same number of bit sequences $\hat{x}$. By employing this scheme, it offers better performance in terms of user fairness due to the coexistence mechanism for OMA and NOMA. Consequently, the uplink performance of the far user UE_a will be improved.

B. TRANSMISSION OF SYMBOL-MATCH SCHEME

Except for adopting the bit sequences of the same size, the symbols sequences of the same size can also be considered, as illustrated in Fig. 4 (b). In this situation, two users have bit sequences of different sizes. Thus, compared with the bit-match scheme, these bit sequences occupy fewer RBs when transferring the same amount of data. Therefore, different from the bit-match scheme, the symbol-match scheme has a better spectral efficiency since NOMA is independently implemented in the uplink. However, due to the different sizes of the bit sequences at the BS, the bit sequence of UE_a has to make up the missing part with zero-padding for an intact XOR operation.

V. NUMERICAL RESULTS

In this section, simulations are carried out to evaluate the performance of the proposed model Hybrid-TWRS. We first reveal the differences between the bit-match scheme and the symbol-match scheme. Then the simulation results are used to compare the BER/BLER performance and the throughput of the three systems.

A. BIT-MATCH SCHEME AND SYMBOL-MATCH SCHEME ANALYSIS

To verify the analysis in section IV and select an appropriate scheme for the proposed model, numerical simulations are carried out to reveal the differences between the two schemes. Simulation parameters are summarized in Table 2. The SNR are defined as $\text{SNR}_a = P_a|h_a|^2/P_n$ and $\text{SNR}_b = P_b|h_b|^2/P_n$ respectively. Without loss of generality, in our simulations, the SNR gap between the two users are designed as: $\tau = \text{SNR}_b - \text{SNR}_a = 6\text{dB}$. Besides, the deviation of $P_a|h_a|$ and $P_b|h_b|$ is set as 25% in maximum.

TABLE 2. Simulation parameters.

Modulation	BPSK (UE_a), QPSK (UE_b)
Power allocation factor in downlink NOMA	0.9 (UE_a), 0.1 (UE_b) [24]
Coding rate	1/3; LTE Turbo
Channel model	Rayleigh flat
Number of multiplexed UEs	1 (OMA), 2 (NOMA)
Detection algorithm	MMSE-SIC (NOMA)/ MMSE (OMA, NC)
Number of simulated bit in a subframe	1024
Number of simulated subframe	$1*10^6$ (uplink)/ $5*10^6$ (system-level)

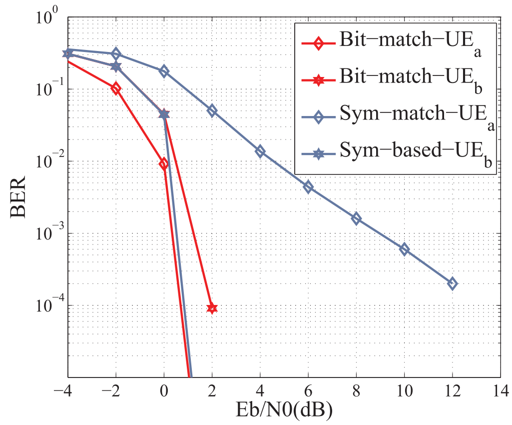

FIGURE 5. Uplink BER performance comparison of different transmission schemes in Hybrid-TWRS.

Fig. 5 shows the BER performance of the two schemes in the uplink Hybrid-TWRS. For the bit-match scheme, the BER of UE_a is better than that of UE_b owing to the coexistence for OMA and NOMA. Moreover, with the similar BER performance of UE_b in both two schemes, we can find that the average BER of the bit-match scheme is superior to that of the symbol-match scheme. However, compared with the symbol-match scheme, the bit-match scheme has its restriction on throughput in the uplink, which can be seen in Fig. 6. Due to the independent NOMA technique, the uplink throughput of the symbol-match scheme is higher than that of the bit-match scheme. Note that we set the bottom x-axis of Fig. 6, Fig. 7, and Fig. 8 as the SNR of UE_b.

From the perspective of the system level, we consider the overall impact of different transmission schemes on the Hybrid-TWRS. Fig. 7 compares the performance of the two schemes in terms of the average BER. It can be observed that a better performance gain is acquired when the bit-match scheme is applied. In Fig. 8, as we mentioned before, the symbol-match scheme has the strength of high spectral efficiency, which is reflected in the uplink throughput

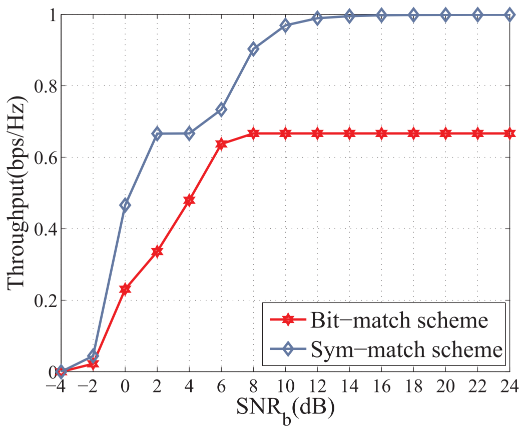

FIGURE 6. Uplink throughput performance comparison of different transmission schemes in Hybrid-TWRS.

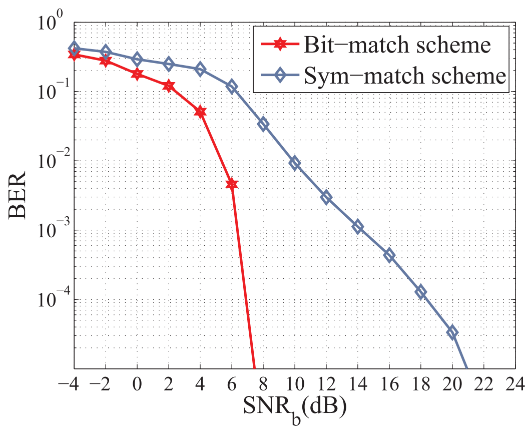

FIGURE 7. System-level BER performance comparison of different transmission schemes in Hybrid-TWRS.

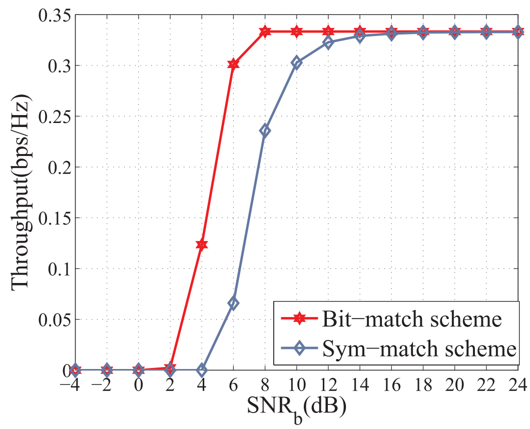

FIGURE 8. System-level throughput performance comparison of different transmission schemes in Hybrid-TWRS.

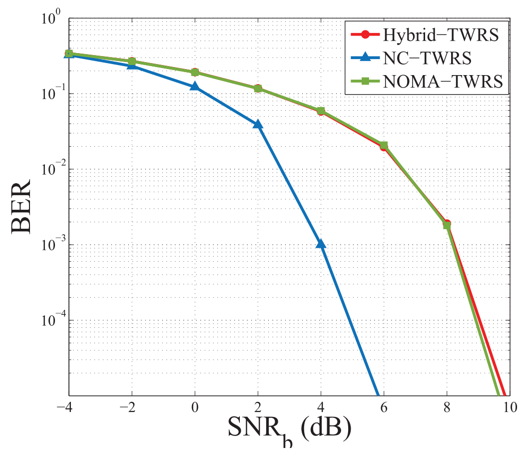

FIGURE 9. Uplink BER performance comparison of different methods.

performance. However, the operation for downlink network coding at the BS takes that advantage away. The reason is that for channel reciprocity, the network coded bit sequence needs to adopt the same modulation method as the far user UE_a. According to the above, the symbol-match scheme loses its superiority in throughput, which can be observed in Fig. 8.

The comparison of the two schemes in the proposed model Hybrid-TWRS can be summarized as follows.

(1) In the uplink and the entire system, the BER performance of the bit-match scheme is better than that of the symbol-match scheme.

(2) At the system level, the throughput performance of the two schemes becomes closer with the rise of SNR until they become equal when SNR = 16 dB.

Based on the above, we prefer to choose the bit-match scheme for our proposed model.

B. THE PROPOSED TWO-WAY RELAYING ANALYSIS

In this subsection, simulations are carried out to compare the performance of our proposed two-way relaying system Hybrid-TWRS versus the methods of NC-TWRS and NOMA-TWRS. We simulate a two-way relaying with a base station located in the center of the network, and two terminal users are distributed in this coverage range. Simulation parameters are also summarized in Table 2. For a fair comparison, the transmitted power of each technique is set to the same, and all three methods experience Rayleigh flat fading channels. The SNR gap between the two users is designed to be the same as in the previous subsection, i.e., $\tau = \text{SNR}_b - \text{SNR}_a = 6$dB. Also note that the bottom x-axis in the simulation results represent the SNR of user UE_b (i.e., the near user).

Fig. 9 illustrates the uplink BER comparison of Hybrid-TWRS and two other counterparts NC-TWRS and NOMA-TWRS. It is observed that the uplink BER performance of Hybrid-TWRS and NOMA-TWRS is basically the same because they both utilize the NOMA scheme. Additionally, the uplink BER performance of NC-TWRS is superior to those of Hybrid-TWRS and NOMA-TWRS, but at the expense of reduced spectral efficiency. Specifically, instead of occupying the same RB in NOMA scheme, the OMA scheme occupies two orthogonal resources for two users, respectively. This effect can be observed in the following simulation of system throughput. For NOMA, we believe that the error propagation of the signals caused by the application of SIC technique is the main reason for its poor performance in

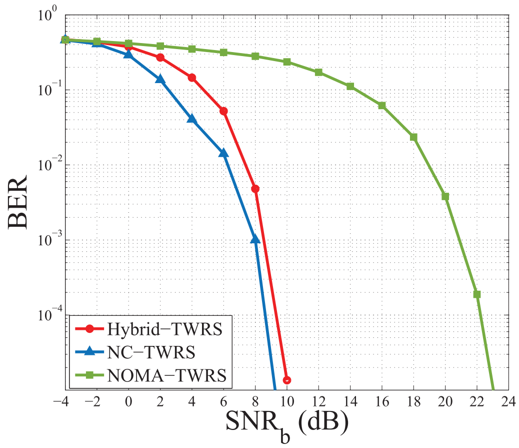

FIGURE 10. System-level BER comparison of different methods.

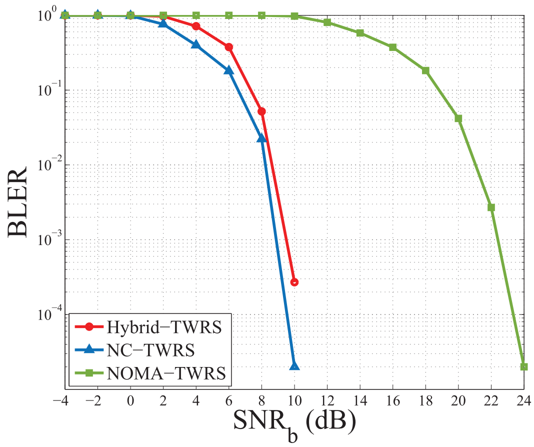

FIGURE 11. System-level BLER performance comparison of different methods.

comparison with OMA. The details are given in the following paragraph describing Fig. 11.

Note that in Fig. 10, the system-level BER performance comparison of Hybrid-TWRS and two other methods is studied. Comparing Hybrid-TWRS to NOMA-TWRS, due to the application of the downlink network coding instead of the NOMA scheme, the XOR operation on Hybrid-TWRS has a better BER/BLER performance than the direct superposition on NOMA-TWRS. Hence it seems that Hybrid-TWRS has a considerable performance advantage over NOMA-TWRS. Besides, Fig. 10 also shows that the system-level BER of NC-TWRS is still better than that of Hybrid-TWRS for its benefits from the OMA scheme applied in the uplink.

The system-level BLER performance comparisons of the three methods are demonstrated in Fig. 11. It can be seen that the performances of Hybrid-TWRS and NC-TWRS are quite better than that of NOMA-TWRS. Given that the uplink BER between Hybrid-TWRS and NOMA-TWRS is basically the same, the error propagation caused by the SIC technique applied in downlink NOMA-TWRS is the main reason for its poor performance. Particularly, the signal of the first detected user is recovered directly from the original received signal with SIC; while for the second detected user, its signal is

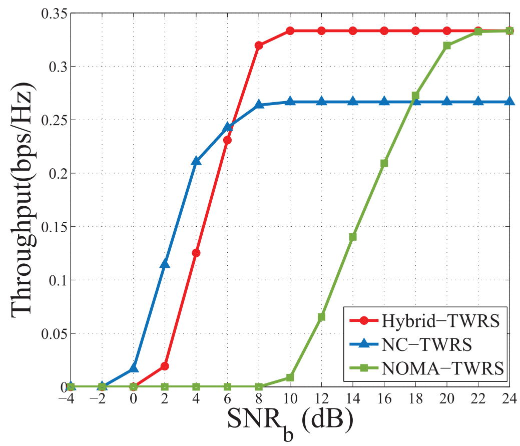

FIGURE 12. System throughput comparison of different methods.

reconstructed from the received signal which subtracts the signal of the first detected user. If the first detected user is detected erroneously, obviously the decoding of its signal will be incorrect. Furthermore, the accuracy of the decoding will also affect the performance of the second detected user.

In addition, Fig. 12 illustrates the system throughput of all three methods and reveals perfect consistency between the derivation and simulations. Firstly, the system throughput increases with the SNR, which follows the intuition that low BLER contributes to high throughput. Moreover, NC-TWRS achieves higher system throughput compared to Hybrid-TWRS at lower SNR condition. The reason is that the effect of error propagation caused by SIC in NOMA dominates the system performance at lower SNR. However, with the increase of SNR, the throughput of Hybrid-TWRS can eventually exceed that of NC-TWRS, that is because when SNR is high enough, the high spectral efficiency brought by non-orthogonal resources dominates the system performance. According to the above analysis, an adaptive scheme for OMA and NOMA in the uplink can be considered in this paper. In particular, in order to improve network performance, we can consider using NC-TWRS instead of Hybrid-TWRS when SNR is low. Then, we can also switch to Hybrid-TWRS at sufficiently high SNR.

Fig. 12 also shows that at lower SNR, the system throughput of Hybrid-TWRS is much higher than that of NOMA-TWRS. The reason is that, compared with the direct superposition, the XOR operation of Hybrid-TWRS is able to avoid the influence of inter-user interference between two users. Therefore, the error propagation has less impact on Hybrid-TWRS. Furthermore, when non-orthogonal resources dominate the system performance at higher SNR, the system throughput of NOMA-TWRS becomes consistent with that of Hybrid-TWRS since the users in both two methods occupy the same number of RBs.

In addition, we also investigate how the throughput performance of the three two-way relaying systems behave when the SNR gap between two users τ is changed. As shown in Fig. 13, we change the SNR gap from 4 dB to 8 dB

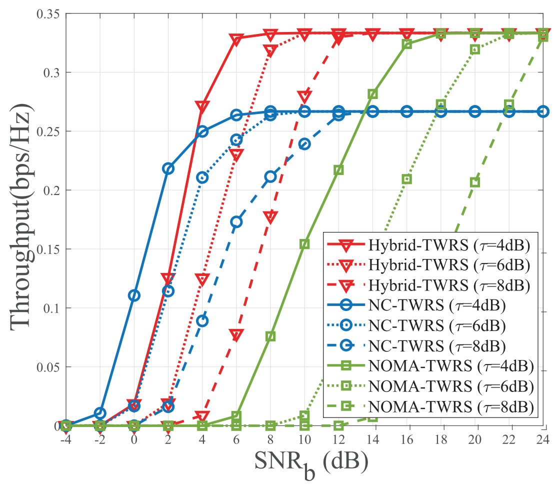

FIGURE 13. System throughput comparison of different methods with different SNR gaps τ.

TABLE 3. Detection complexity for uplink and downlink.

	real-valued multiplications	real-valued additions
$\mathbf{H}^H\mathbf{H}$	$2UV + \frac{4U(V^2-V)}{2}$	$(2U-1)V + \frac{(4U-2)(V^2-V)}{2}$
$((\cdot)+\mathbf{I}N_0)$	–	$2V$
$(\cdot)^{-1}$	$2V^3+6V^2$	$2V^3+2V^2$
$(\cdot)^{-1}\mathbf{H}^H$	$4UV^2$	$4UV^2-2UV$

with a step of 2 dB. Now two new simulation scenarios are considered together with the former case $\tau = 6$ dB. It can be observed that in $\tau = 4$ dB, 6 dB and 8 dB cases, the throughput comparison of the three systems has the same result. Also, the reason for this result is consistent with the analysis in the Fig. 12. However, the impact of different SNR gaps on a particular system is quite large. It can be found that the throughput performance of a particular system increases with the rise of τ. Such phenomenon is reasonable, because with the increasing τ, the power of the far user will be strengthened. Consequently, it is easier to achieve a correct decoding for far user when it is first decoded in the downlink SIC receiver. Thus, the error propagation effect is weakened and the system throughput performance is improved.

As we mentioned in the above analysis, despite the numerous benefits of NOMA over OMA, the issues such as error propagation and inter-cell interference are still the key factor limiting the performance of NOMA scheme, which renders the following two challenges in future two-way relay networks: (i) the characterisation of inter-user interference (IUI) caused by different asymmetric channels should be considered; (ii) a dynamic allocation of MCS is needed for NOMA user pairs to adapt to the IUI [25], [26].

VI. CONCLUSION

In this paper, a hybrid two-way relaying method Hybrid-TWRS is introduced. Compared with the conventional two-way relaying system NC-TWRS, Hybrid-TWRS significantly improves system throughput by further exploiting the multiplexing gain of resources. Meanwhile, by utilizing the lossless compressing gain brought by network coding, Hybrid-TWRS achieves a better BER/BLER performance compared with NOMA-based two-way relaying system NOMA-TWRS. Moreover, the detection complexity of Hybrid-TWRS is lower than that of NOMA-TWRS, which achieves savings in the computational resources. In addition, the transmission schemes of Hybrid-TWRS are investigated. By exploring both the multiplexing gain of NOMA and the compressing gain of network coding, the hybrid concept of Hybrid-TWRS is proved to be a promising technology. For future research, by focusing on adaptive modulation and coding (AMC) for NOMA user pairs, more results could possibly be found out for two-way relay networks.

APPENDIX A

A. PROOF FOR THE DETECTION COMPLEXITY

For MMSE detection algorithm, its weighted matrix is formulated as

$$W_{MMSE} = (\mathbf{H}^H\mathbf{H} + \mathbf{I}N_0)^{-1}\mathbf{H}^H, \tag{39}$$

where $\mathbf{H} \in \mathbb{C}^{(U\times V)}$ denotes the channel matrix, with N_0 being the power spectral density. Due to the complexity of $\mathbf{H}^H\mathbf{H}$ by using the Hermitian structure of the product $\mathbf{H}^H\mathbf{H} \in \mathbb{C}^{(V\times V)}$ [21], the strictly lower triangular part of $\mathbf{H}^H\mathbf{H}$ need not be computed since it corresponds to the Hermitian of the strictly upper triangular part. For this reason, we have to compute only the V main diagonal entries of $\mathbf{H}^H\mathbf{H}$ and the $\frac{V^2-V}{2}$ upper off-diagonal entries.

Besides, according to [21], each entry requires an inner product step $\boldsymbol{a}^H\boldsymbol{b}$ costing U multiplications and $U-1$ summations, where vectors $\boldsymbol{a} \in \mathbb{C}^V$ and $\boldsymbol{b} \in \mathbb{C}^V$ have dimension V. For $\boldsymbol{a}^H\boldsymbol{b}$, the number of real-valued multiplications and real-valued summations are $4U$ and $4U-2$, respectively. Note that this is only suitable for upper off-diagonal elements. For main diagonal entries of $\mathbf{H}^H\mathbf{H}$, since it is the result of a complex vector multiplied by a conjugate transpose of a complex vector, its number of operations is half of the upper off-diagonal elements. Hence, the number of real-valued multiplications and real-valued summations for main diagonal entries of $\mathbf{H}^H\mathbf{H}$ are $2U$ and $2U-1$, respectively.

Consequently, the number of real-valued multiplications for $\mathbf{H}^H\mathbf{H}$ is $2UV + \frac{4U(V^2-V)}{2}$, the number of real-valued summations for $\mathbf{H}^H\mathbf{H}$ is $(2U-1)V + \frac{(4U-2)(V^2-V)}{2}$. Applying the similar way, other terms of weighted matrix W_{MMSE} can also be derived. The complexity is presented in Table 3.

In this paper, $\mathbf{H}$ satisfies $\mathbf{H} \in \mathbb{C}^{(1\times N)}$, where N is denoted as the number of detected symbols in a simulation frame. By substituting the constraints of $\mathbf{H}$ to the above table, and further summarizing the result of the four terms, the complexity of MMSE algorithm can be finally obtained.

In summary, the complexity of MMSE detection algorithm is $2N^3 + 12N^2$ for multiplications and $2N^3 + 7N^2$ for additions.

REFERENCES

[1] L. Dai, B. Wang, Z. Ding, Z. Wang, S. Chen, and L. Hanzo, "A survey of non-orthogonal multiple access for 5G," *IEEE Commun. Surveys Tuts.*, vol. 20, no. 3, pp. 2294–2323, 3rd Quart., 2018.

[2] Z. Ding, J. Xu, O. A. Dobre, and V. Poor, "Joint power and time allocation for NOMA–MEC offloading," *IEEE Trans. Veh. Technol.*, vol. 68, no. 6, pp. 6207–6211, Jun. 2019.
[3] J. Zhao, Y. Liu, K. K. Chai, Y. Chen, and M. Elkashlan, "Joint subchannel and power allocation for NOMA enhanced D2D communications," *IEEE Trans. Commun.*, vol. 65, no. 11, pp. 5081–5094, Nov. 2017.
[4] M. Vaezi, Z. Ding, and H. V. Poor, *Multiple Access Techniques for 5G Wireless Networks and Beyond*. Cham, Switzerland: Springer, 2018.
[5] S. M. R. Islam, N. Avazov, O. A. Dobre, and K.-S. Kwak, "Power-domain non-orthogonal multiple access (NOMA) in 5G systems: Potentials and challenges," *IEEE Commun. Surveys Tuts.*, vol. 19, no. 2, pp. 721–742, 2nd Quart., 2017.
[6] Y. Saito, Y. Kishiyama, A. Benjebbour, T. Nakamura, A. Li, and K. Higuchi, "Non-orthogonal multiple access (NOMA) for cellular future radio access," in *Proc. IEEE VTC Spring*, Jun. 2013, pp. 1–5.
[7] Z. Ding, P. Fan, and H. V. Poor, "Impact of user pairing on 5G non-orthogonal multiple-access downlink transmissions," *IEEE Trans. Veh. Technol.*, vol. 65, no. 8, pp. 6010–6023, Aug. 2016.
[8] Y. Saito, A. Benjebbour, Y. Kishiyama, and T. Nakamura, "System-level performance evaluation of downlink non-orthogonal multiple access (NOMA)," in *Proc. IEEE Int. Symp. Pers., Indoor Mobile Radio Commun. (PIMRC)*, Sep. 2013, pp. 611–615.
[9] L. Zhu, J. Zhang, Z. Xiao, X. Cao, and D. O. Wu, "Optimal user pairing for downlink non-orthogonal multiple access (NOMA)," *IEEE Wireless Commun. Lett.*, vol. 8, no. 2, pp. 328–331, Apr. 2019.
[10] B. Rankov and A. Wittneben, "Achievable rate regions for the two-way relay channel," in *Proc. IEEE ISIT*, Jul. 2006, pp. 1668–1672.
[11] S. Zhang, F. Gao, and C. X. Pei, "Optimal training design for individual channel estimation in two-way relay networks," *IEEE Trans. Signal Process.*, vol. 60, no. 9, pp. 4987–4991, Sep. 2012.
[12] R. Ahlswede, N. Cai, S.-Y. R. Li, and R. W. Yeung, "Network information flow," *IEEE Trans. Inf. Theory*, vol. 46, no. 4, pp. 1204–1216, Jul. 2000.
[13] S. T. Başaran, G. K. Kurt, M. Uysal, and I. Altunbaş, "A tutorial on network coded cooperation," *IEEE Commun. Surveys Tuts.*, vol. 18, no. 4, pp. 2970–2990, 4th Quart., 2016.
[14] S. Gokceli, H. Alakoca, S. T. Basaran, and G. K. Kurt, "OFDMA-based network-coded cooperation: Design and implementation using software-defined radio nodes," *EURASIP J. Adv. Signal Process.*, vol. 2016, no. 1, p. 8, Dec. 2016.
[15] F. Khalid and S. Jangsher, "Upper bound of capacity for a MU-MIMO NOMA in a two way relaying network," in *Proc. WINCOM*, Oct. 2018, pp. 1–6.
[16] B. Zheng, M. Wen, C.-X. Wang, X. Wang, F. Chen, J. Tang, and F. Ji, "Secure NOMA based two-way relay networks using artificial noise and full duplex," *IEEE J. Sel. Areas Commun.*, vol. 36, no. 7, pp. 1426–1440, Jul. 2018.
[17] X. Yue, Y. Liu, S. Kang, A. Nallanathan, and Y. Chen, "Modeling and analysis of two-way relay non-orthogonal multiple access systems," *IEEE Trans. Commun.*, vol. 66, no. 9, pp. 3784–3796, Sep. 2018.
[18] K. Higuchi and A. Benjebbour, "Non-orthogonal multiple access (NOMA) with successive interference cancellation for future radio access," *IEICE Trans. Commun.*, vols. E98–B, no. 3, pp. 403–414, Mar. 2015.
[19] D. Tse and P. Viswanath, *Fundamentals of Wireless Communication*. Cambridge, U.K.: Cambridge Univ. Press, 2005.
[20] Y. Liu, Z. Qin, M. Elkashlan, Z. Ding, A. Nallanathan, and L. Hanzo, "Non-orthogonal multiple access for 5G and beyond," *Proc. IEEE*, vol. 105, no. 12, pp. 2347–2381, Dec. 2017.
[21] R. Hunger, *Floating Point Operations in Matrix-Vector Calculus*. München, Germany: Technische Universität München, 2005.
[22] *Technical Specification Group Radio Access Network; Evolved Universal Terrestrial Radio Access (E-UTRA); Physical Layer Procedures (Release 15), V15.1.0*, document TS 36.213, 3GPP, Mar. 2018.
[23] E. C. Cejudo, H. Zhu, and O. Alluhaibi, "On the power allocation and constellation selection in downlink NOMA," in *Proc. IEEE 86th Veh. Technol. Conf.*, Sep. 2017, pp. 1–5.
[24] Z. Yang, Z. Ding, P. Fan, and N. Al-Dhahir, "A general power allocation scheme to guarantee quality of service in downlink and uplink NOMA systems," *IEEE Trans. Wireless Commun.*, vol. 15, no. 11, pp. 7244–7257, Nov. 2016.
[25] X. Wang, F. Labeau, and L. Mei, "Closed-form BER expressions of QPSK constellation for uplink non-orthogonal multiple access," *IEEE Commun. Lett.*, vol. 21, no. 10, pp. 2242–2245, Oct. 2017.
[26] S. Kim, H. Kim, and D. Hong, "Joint power allocation and MCS selection in downlink NOMA system," in *Proc. IEEE PIMRC*, Sep. 2018, pp. 1–4.

FANBO WEI received the B.S. degree in communication engineering from the University of Electronic Science and Technology of China (UESTC), Chengdu, China, in 2017. He is currently pursuing the M.S. degree with the Shanghai Advanced Research Institute, Chinese Academy of Sciences, Shanghai, China. His research interest includes wireless communications with focus on multiple access technique for the next generation wireless networks.

TING ZHOU received the B.S. and M.S. degrees from the Department of Electronic Engineering, Tsinghua University, in 2004 and 2006, respectively, and the Ph.D. degree from the Shanghai Institute of Microsystem and Information Technology (SIMIT), Chinese Academy of Sciences (CAS), in 2011. She is currently a Full Professor with the Shanghai Advanced Research Institute, CAS. She has coauthored more than 20 technical journals and conference, and holds 49 granted or filed patents. Her research interests include wireless resource management and mobility management and intelligent networking of heterogeneous wireless networks and 5G mobile systems. She received the 2015 and 2016 First Prize of Technological Invention Award from the China Institute of Communications and the 2015 Second Prize of Shanghai Science and Technology Progress Award.

TIANHENG XU (S'14–M'16) received the Ph.D. degree from the Shanghai Institute of Microsystem and Information Technology, Chinese Academy of Sciences, Shanghai, China, in 2016. He is currently an Associate Professor with the Shanghai Advanced Research Institute, Chinese Academy of Sciences. His main research interests include 5G wireless communications, spectrum sensing technologies, statistical signal transmission technologies, and vehicular communication technologies. He received the President Scholarship of Chinese Academy of Sciences (First Grade), in 2014, the Outstanding PhD Graduates Award of Shanghai, in 2016. He also received the Best Paper Award from the IEEE GlobeCom 2016.

HONGLIN HU (SM'13) received the Ph.D. degree in communications and information system from the University of Science and Technology of China, China, in 2004. He was with Future Radio, Siemens AG Communications, Germany. From 2015 to 2018, he was a Finland Distinguished Professor (FiDiPro) with the VTT Technical Research Centre of Finland, Finland. Since 2009, he has been a Full Professor with the Shanghai Institute of Microsystem and Information Technology, Chinese Academy of Sciences, China. Since 2013, he has also been an Adjunct Professor with ShanghaiTech University, China, and the Vice Director of the Shanghai Research Center for Wireless Communications, China. Since 2016, he has been with the Shanghai Advanced Research Institute, Chinese Academy of Sciences, China. He was a recipient of the 2016 IEEE Jack Neubauer Memorial Award (the Best Paper Award of the IEEE Transactions on Vehicular Technology) and the Best Paper Award from the IEEE GlobeCom 2016. He was the Vice Chair of the IEEE Shanghai Section. He was a leading Guest Editor for the IEEE Wireless Communications special issue on Mobile Converged Networks and the *IEEE Communications Magazine* special issue on Software Defined Wireless Networks (Part I and Part II).